www.lajss.org
Latin American Journal of Solids and Structures 3 (2006) 393–415

Damage location in flexible structures using H_2 and H_∞ norm approaches

Douglas Domingues Bueno, Clayton Rodrigo Marqui and Vicente Lopes Junior*

Department of Mechanical Engineering, Universidade Estadual Paulista – UNESP
Ilha Solteira, SP – Brazil

Abstract

Nowadays there is great interest in structural damage detection using non- destructive tests. Once the failure is identified, as for instance a crack, it is possible to plan the next step based on a predictive maintenance program. There are several different approaches that can be used to obtain information about the existence, location and extension of the fault in mechanical systems by non destructive tests. Among these methodologies, one can mention different optimization techniques, as for instance classical methods, genetic algorithms, artificial neural networks, etc. Most of these techniques, which are based on element-by-element adjustments of a finite element (FE) model, take advantage of the dynamic behavior of the system. These approaches are known as parameter updating methods, and are well described in the literature. The main goal of this paper is to use H_2 and H_∞ norms to obtain damage locations information. The proposal allows the identification of damaged elements in the structure, and provides information about the influence of these damages on the natural modes of the system. The paper concludes with a numerical simulation in an aluminum plate represented by a model of second order written in modal coordinates. Four structural damage cases were simulated using stiffness reduction. The results show with clarity the localization of each simulated damage; so, proving the viability of the presented methodology.

Keywords: damage location, PVDF sensors, PZT actuators, predictive maintenance, system norms, H_2 and H_∞ norm.

1 Introduction

Structural Health Monitoring (SHM) denotes a system with the ability to detect and interpret adverse "changes" in a structure. The aim of this program is to improve reliability and reduce life-cycle costs. There are several advantages for using a SHM system over traditional inspection cycles, such as reduced down-time, elimination of component tear-down inspections and the potential prevention of failure during operation. Aerospace structures have one of the highest investments for SHM applications, since damage can lead to catastrophic and expensive failures, and the vehicles involved undergo regular costly inspections. Currently 27% of an average

*Corresp. author email: vicente@dem.feis.unesp.br Received 22 May 2006; In revised form 13 September 2006

aircraft's life cycle cost, both for commercial and military vehicles, is spent on inspections and repairs. This cost excludes the opportunity cost associated with the time the aircraft is grounded for scheduled maintenance [15].

New materials have been investigated for damage characterization in mechanical structures using specific SHM program. Most popular are the ones that show the piezoelectric effect, in special the ceramics, PZT (*Lead Zirconate Titanate*) and plastic films, PVDF (*PolyVinyliDeno Floride*). Piezoelectric materials develop an electric field when submitted to a force (*direct effect*) and present a deformation when are submitted to an electric field (*inverse effect*). Generally, PVDF's are used as sensors for being malleable and to admit complex forms [13]. Damage location using PVDF sensors based on methods of vibration analysis consists basically of monitoring parameters that characterize the condition of structures or machines (predictive maintenance). Many authors use PZT and PVDF material for damage locations in mechanical structures. Inman proposes the use of intelligent materials (piezoelectric material) combined with control techniques in order to form a self-healing structure [7].

Different approaches have been proposed for SHM, as for instance, passive control technique and piezoelectric materials can be combined to detect damage [11]. In this method, the natural frequencies of the system are identified to detect damage in a closed loop system, and the stability is ensured. System's damping usually increases when a virtual passive controller is added. Another branch of research investigates evolutionary algorithm based on natural observation, as for instance, artificial neural networks, genetic algorithm, simulated annealing, particle swarm optimization, etc. Techniques based on neural networks require a model in the training process to be able to detect damage [5], or sufficient amount of data that represent very well every damage situation under analysis [17]. Neural networks have been used to investigate damage detection in composite ship hulls [3]. The authors developed a Finite Element model for a stiffened plate to simulate dynamic response of the structure with and without damage, and the technique was successfu1 for identifying crack length and location on the faceplate.

Adaptive on-line control algorithm was used for both vibration suppression and damage detection [16]. The method was demonstrated on a simulated three degree of freedom system with an actuator. Large control efforts are required when an abrupt change in system properties occur, as the controller attempts to compensate and return the monitored responses to their initial values. These efforts may, therefore, be used as indicators of damage.

Modal and sensor norms also can be used to determine damage locations [21]. Following this branch of research that has a small amount of related work in the literature, the present paper proposes the use of H_2 and H_∞ norms to characterize damage in flexible structures. This approach localizes damaged elements in the structure, and also provides information about the changes in the natural modes of the damaged system. The numerical application considers an aluminum plate represented for a model of second order written in modal coordinates. Four structural damage cases were simulated using stiffness reduction.

The fundamental equations governing the equivalent piezoelectric actuators and sensors are also derived. Piezoelectric finite elements are developed based on shell elements, since any

variation in modal properties can be misinterpreted as damage. Systems that require more sophisticated modeling techniques are considered in the literature [2, 18].

2 Structural modeling

Flexible structures can be represented by a mathematical model in the form of ordinary differential equations involving the input, the output, and possibly some additional variables that are intermediary between the input and output. The standard form of the state equations of a linear time-invariant (LTI) system is given by

$$\begin{aligned} \dot{\mathbf{x}}(t) &= \mathbf{A}\mathbf{x}(t) + \mathbf{B}\mathbf{u}(t) \\ \mathbf{y}(t) &= \mathbf{C}\mathbf{x}(t) + \mathbf{D}\mathbf{u}(t) \end{aligned} \tag{1}$$

where $\mathbf{A}$, $\mathbf{B}$ and $\mathbf{C}$ are the dynamic, input and output matrices, respectively; $\mathbf{x}(t)$, $\mathbf{y}(t)$ and $\mathbf{u}(t)$ are the state vector, output vector and input control vector, respectively, and $\mathbf{D}$ is the input-output coupling matrix, which will be considered zero.

With the representation of the model in the nodal form it is possible to write the system in mass terms, nodal stiffness, damping, displacements and velocity

$$\begin{aligned} \ddot{\mathbf{q}}(t) + \mathbf{M}^{-1}\mathbf{D_a}\dot{\mathbf{q}}(t) + \mathbf{M}^{-1}\mathbf{K}\mathbf{q}(t) &= \mathbf{M}^{-1}\mathbf{B}_0\mathbf{u}(t) \\ \mathbf{y}(t) &= \mathbf{C_{oq}}\mathbf{q}(t) + \mathbf{C_{ov}}\dot{\mathbf{q}}(t) \end{aligned} \tag{2}$$

In this equation $\mathbf{q}(t)$ is the nd x 1 displacement vector, $\mathbf{u}(t)$ is the s x 1 input vector, $\mathbf{y}(t)$ is the output vector, r x 1, $\mathbf{M}$ is the mass matrix, nd x nd, $\mathbf{D}_a$ is the damping matrix, nd x nd, and $\mathbf{K}$ is the stiffness matrix, nd x nd. The input matrix $\mathbf{B}_0$ is nd x s, the output displacement matrix $\mathbf{C}_{oq}$is r x nd, and output velocity matrix $\mathbf{C}_{ov}$ is r x nd. The mass matrix is positive definite, and the stiffness and damping matrices are positive semi definite, nd is the number of degrees of freedom of the system (linearly independent coordinates describing the finite-dimensional structure), r is the number of outputs and s is the number of inputs.

Through the classic procedure of modal analysis [18], it is possible to write the motion equations in modal coordinates, $\mathbf{q}_m(t)$. Thus, the modal model of second order is given in its final form

$$\begin{aligned} \mathbf{q}(t) &= \mathbf{\Phi}\mathbf{q_m}(t) \\ \ddot{\mathbf{q}}_\mathbf{m}(t) + 2\mathbf{Z}\mathbf{\Omega}\dot{\mathbf{q}}_\mathbf{m}(t) + \mathbf{\Omega}\mathbf{q_m}(t) &= \mathbf{B_m}\mathbf{u}(t) \\ \mathbf{y}(t) &= \mathbf{C_{mq}}\mathbf{q_m}(t) + \mathbf{C_{mv}}\dot{\mathbf{q}}_\mathbf{m}(t) \end{aligned} \tag{3}$$

where Φ is the modal matrix and $\mathbf{Z}$ is the coefficients damping modal matrix (ζ_i)

$$\begin{aligned} \mathbf{\Omega}^2 &= \mathbf{M_m^{-1}}\mathbf{K_m} \\ \mathbf{Z} &= 0.5\mathbf{M_m^{-1}}\mathbf{D_m}\mathbf{\Omega}^{-1} = 0.5\mathbf{M_m^{-1/2}}\mathbf{K_m^{-1/2}}\mathbf{D_m} \end{aligned} \tag{4}$$

where Ω is the natural frequencies matrix.

The matrices $\mathbf{M}_m$, $\mathbf{K}_m$ and $\mathbf{D}_m$ are diagonals modal matrices of mass, stiffness and damping, respectively. These matrices are given by

$$\begin{aligned} \mathbf{M_m} &= \mathbf{\Phi}^T \mathbf{M} \mathbf{\Phi} \\ \mathbf{K_m} &= \mathbf{\Phi}^T \mathbf{K} \mathbf{\Phi} \\ \mathbf{D_m} &= \mathbf{\Phi}^T \mathbf{D_a} \mathbf{\Phi} \end{aligned} \tag{5}$$

Matrix $\mathbf{D}_a$ is assumed to be proportional to mass and stiffness matrices.

$$\mathbf{D_a} = \alpha \mathbf{M} + \beta \mathbf{K} \tag{6}$$

Matrix $\mathbf{B}_m$ in Eq. (3) is the input modal matrix, or participation modal matrix and is given by

$$\mathbf{B_m} = \mathbf{M_m^{-1}} \mathbf{\Phi}^T \mathbf{B_0} \tag{7}$$

$\mathbf{C}_{mq}$ e $\mathbf{C}_{mv}$ are the output displacement and velocity modal matrices

$$\begin{aligned} \mathbf{C_{mq}} &= \mathbf{C_{oq}} \mathbf{\Phi} \\ \mathbf{C_{mv}} &= \mathbf{C_{ov}} \mathbf{\Phi} \end{aligned} \tag{8}$$

The state equation, usually written in a vector-matrix format, allows the equations to be manipulated more easily. In this format the preceding matrices become

$$\mathbf{A} = \begin{bmatrix} \mathbf{0} & \mathrm{I} \\ -\Omega^2 & -2\mathbf{Z}\Omega \end{bmatrix}, \quad \mathbf{B} = \begin{bmatrix} \mathbf{0} \\ \mathbf{B}_{\mathrm{m}} \end{bmatrix}, \quad \mathbf{C} = \begin{bmatrix} \mathbf{C}_{\mathrm{mq}} & \mathbf{C}_{\mathrm{mv}} \end{bmatrix} \tag{9}$$

The modal state-space realization is characterized by the block-diagonal dynamic matrix and the related input and output matrices [12].

$$\mathbf{A}_m = \mathrm{diag}\left(\mathbf{A}_{\mathrm{mi}}\right), \qquad \mathbf{B}_m = \begin{bmatrix} \mathrm{B_{m1}} \\ \mathrm{B_{m2}} \\ \vdots \\ \mathrm{B_{mn}} \end{bmatrix}, \qquad \mathbf{C}_m = \begin{bmatrix} \mathbf{C}_{\mathrm{m1}} & \mathbf{C}_{\mathrm{m2}} & \cdots & \mathbf{C}_{\mathrm{mn}} \end{bmatrix} \tag{10}$$

where i=1,2,...,n, $\mathbf{A}_{mi}$, $\mathbf{B}_{mi}$ and $\mathbf{C}_{mi}$ are 2 x 2, 2 x s and r x 2 blocks, respectively.

These blocks can be obtained by several different forms and also it is possible to convert in another realization through a linear transformation. One possible form to block $\mathbf{A}_{mi}$ can be written by

$$\mathbf{A}_{\mathrm{mi}} = \begin{bmatrix} -\zeta_i \omega_i & \omega_i \\ -\omega_i(\zeta_i^2 - 1) & -\zeta_i \omega_i \end{bmatrix} \tag{11}$$

The state vector $\mathbf{x}(t)$ of the modal coordinates system consists of n independent components, $\mathbf{x}_i(t)$, that represent a state of each mode. The $\mathbf{x}_i(t)$ (ith state component), related to Eq. (11), is defined by [19]

$$\mathbf{x}_i(t) = \begin{Bmatrix} \mathbf{q}_{\mathrm{mi}}(t) \\ \mathbf{q}_{\mathrm{moi}}(t) \end{Bmatrix}, \quad \textit{where } \mathbf{q}_{\mathrm{moi}}(t) = \zeta_i \mathbf{q}_{\mathrm{mi}}(t) + \dot{\mathbf{q}}_{\mathrm{mi}}(t)/\omega_i \tag{12}$$

3 H_2 norm index for damage location

Norms of systems are as measure of size and can be used for diverse applications. It can be detached the use for damage locations [21], reduction of models [8,20], control [4,10] and optimal placement of sensors and actuators [9,19].

Considering ($\mathbf{A}$, $\mathbf{B}$, $\mathbf{C}$) the representation in space of states of a system where the transfer function G is given by

$$G(\omega) = \mathbf{C}(j\omega\mathbf{I} - \mathbf{A})^{-1}\mathbf{B} \tag{13}$$

where ω is the excitation frequency. The H_2 norm of the system is defined by

$$||G||_2^2 = \frac{1}{2\pi}\int_{-\infty}^{+\infty} tr(G^T(\omega)G(\omega))d\omega \tag{14}$$

where tr is the trace of the matrix.

A convenient way to calculate the value of the norm is to consider ($\mathbf{A}_i$, $\mathbf{B}_i$, $\mathbf{C}_i$) the representation in space of states of the ith mode of the system. Using this representation it is possible to approach the H_2 norm by [19]

$$||G_i||_2 \cong \frac{||\mathbf{B}_i||_2||\mathbf{C}_i||_2}{2\sqrt{\zeta_i\omega_i}} \cong \frac{||\mathbf{B}_i||_2||\mathbf{C}_i||_2}{\sqrt{2\Delta\omega_i}} \tag{15}$$

where $\Delta\omega_i$ is defined as a half-power frequency at the ith resonance, $\Delta\omega_i = 2\zeta_i\omega_i$ [6].

The H_2 norm of the system is the RMS sum of all modes. The H_2 norm with more than one actuator, or sensor, is the RMS sum of the norms for the system with each one of them separately.

$$\|G\|_2 = \sqrt{\sum_{i=1}^{n} ||G_i||_2^2} \tag{16}$$

where n is the number of modes. It is denoted the jth sensor norm of the healthy structure by $||\mathrm{G}_{shj}||_2$, and the jth sensor norm of the damaged structure by $||\mathrm{G}_{sdj}||_2$. The jth sensor index to characterize structural damages is defined as a weighted difference between the jth sensor norm of the healthy and the damaged structure. The sensor index reflects the impact of the structural damage on the jth sensor [21]

$$\sigma_{sj} = \frac{\left|\|G_{shj}\|_2^2 - \|G_{sdj}\|_2^2\right|}{\|G_{shj}\|_2^2} \tag{17}$$

Similarly, denoting the ith mode norm of the healthy structure by $||\mathrm{G}_{mhi}||_2$, and ith mode norm of the damaged structure by $||\mathrm{G}_{mdi}||_2$. The ith mode index to characterize structural damage

is defined as a weighted difference between the ith mode norm of the healthy and the damaged structure. The ith mode index reflects the impact of the structural damage on the ith mode

$$\sigma_{mi} = \frac{\left| \|G_{mhi}\|_2^2 - \|G_{mdi}\|_2^2 \right|}{\|G_{mhi}\|_2^2} \tag{18}$$

4 H_∞ norm index for damage location

The H_∞ norm of stable system is defined as

$$\|G\|_\infty = \max_\omega \ \sigma_{max}\left(G\left(\omega\right)\right) \tag{19}$$

where $\sigma_{max}(\mathrm{G}(\omega))$ is the largest singular value of $\mathrm{G}(\omega\ )$ [12].

For flexible structures in modal representation the H_∞ norm is expressed in terms of the norms of modes. Considering the ith mode ($\mathbf{A}_i$, $\mathbf{B}_i$, $\mathbf{C}_i$), the H_∞ norm is estimated as:

$$||G_i||_\infty \cong \frac{||\mathbf{B}_i||_2||\mathbf{C}_i||_2}{2\zeta_i\omega_i} \tag{20}$$

The H_∞ norm of a single-input-single-output system is the peak magnitude of the transfer function, in terms of its singular values. Due the independence of the modes, the H_∞ norm of the system is the largest value of the mode norms, i.e.,

$$\|G\|_\infty = \max_i \ \|G_i\|_\infty, \quad i = 1, \cdots, n \tag{21}$$

The H_∞ norm of the ith mode of a structure with r sensors is the RMS sum of the norms in this mode for each sensor separately.

$$\|G_i\|_\infty = \sqrt{\sum_{k=1}^{r} \|G_{ki}\|_\infty^2}, \quad i = 1, \cdots, n \tag{22}$$

The H_∞ norm of the system is given by the RMS sum of all modes. The H_∞ norm for a system with more than an actuator, or sensor, is the RMS sum of the norms for the system with each one of them separately.

Similarly to the previous section, it is defined a damage index of the sensor for H_∞ norm. It represents the impact of damages on the structure due the position of the ith sensor

$$\sigma_{sj} = \frac{\left| \|G_{shj}\|_\infty^2 - \|G_{sdj}\|_\infty^2 \right|}{\|G_{shj}\|_\infty^2} \tag{23}$$

where $||\mathrm{G}_{shj}||_\infty$ denote the H_∞norm of the jth sensor for the healthy structure and $||\mathrm{G}_{sdj}||_\infty$ the H_∞ norm of jth sensor for the damaged structure; $s$is the sensor's number.

The mode index is also defined similarly for H_∞ norm. Eq. (24) reflects the impact of the structural damage in the ith mode

$$\sigma_{mi} = \frac{\left| \|G_{mhi}\|_\infty^2 - \|G_{mdi}\|_\infty^2 \right|}{\|G_{mhi}\|_\infty^2} \tag{24}$$

where $||G_{mhi}||_\infty$ denote the norm of the ith mode for the healthy structure and $||G_{mdi}||_\infty$ the norm of the ith mode of the damaged structure.

5 Finite element modeling considering the electromechanical coupling

The basic idea of the Finite Elements Method consists in using as parameters the nodes variable of a finite number of points previously chosen, called nodes points or, simply, nodes. Effecting this procedure, the displacements "**u**" of a finite element can be written in function of the displacement of the nodes, $\mathbf{u}_i$, using appropriate interpolation functions. This relation is given in matrix form as

$$\mathbf{u} = \mathbf{N}_u \mathbf{u}_i; \quad \dot{\mathbf{u}} = \mathbf{N}_u \dot{\mathbf{u}}_i; \quad \ddot{\mathbf{u}} = \mathbf{N}_u \ddot{\mathbf{u}}_i \tag{25}$$

where $\mathbf{N}_u$ is the matrix that contains the interpolation functions that relate the displacements that occur to the long one of the longitudinal axle with the nodes displacements of the element.

Besides of displacements $\mathbf{u}_i$, also the electric potentials ϕ_i must be considered as nodes variable. Therefore, it can be written by analogy with the displacement in matrix form.

$$\varphi = \mathbf{N}_\varphi \varphi_i \tag{26}$$

where $\mathbf{N}_\phi$ is the matrix that contains the interpolation functions that relate the electric potentials that occur to the long one of the PZT with the nodes potentials of the element.

Usually, Hamilton's principle is used to obtain the motion equations in a system electromechanically connected. The idea in this work was to apply the equations of Lagrange in order to find the motion equations of the piezostructure. In the formulation it is considered the mechanical degrees of freedom (displacements) in each structural element, defined by $\mathbf{u}_i$, and the electric degrees of freedom (electric potentials) defined by φ_i. The Lagrange's equations are given by

$$\frac{\partial}{\partial t}\left(\frac{\partial \mathrm{L}}{\partial \dot{\mathbf{u}}_i}\right) - \frac{\partial \mathrm{L}}{\partial \mathbf{u}_i} = \mathbf{F}^e \tag{27}$$

$$\frac{\partial}{\partial t}\left(\frac{\partial \mathrm{L}}{\partial \dot{\phi}_i}\right) - \frac{\partial \mathrm{L}}{\partial \phi_i} = \mathbf{Q}^e \tag{28}$$

where $\mathbf{F}^e$ is the of applied external forces in the element, $\mathbf{Q}^e$ is the electric charge induced for an electric potential applied in the piezoelectric ceramic and $\mathbf{L}$ is the Lagrangian that is defined as

$$\mathrm{L} = \mathrm{T} - \mathrm{U} + \mathrm{W}_e \tag{29}$$

where $\mathbf{T}$ is the kinetic energy, $\mathbf{U}$ is the potential energy and $\mathbf{W}_e$ denotes the work done by electrical forces. The kinetic energy is written as

$$\mathrm{T} = \iiint_{V_s} \frac{1}{2}\rho_s \ \dot{\mathbf{u}}^T \dot{\mathbf{u}} dV_s + \iiint_{V_p} \frac{1}{2}\rho_p \ \dot{\mathbf{u}}^T \dot{\mathbf{u}} dV_p \tag{30}$$

where ρ is the specific mass (kg/m^3), $\mathbf{u}$ and $\dot{\mathbf{u}}$ are displacement and velocity vectors, respectively, and V the volume (m^3). The superscript T means transposed and the subscripts s and p are relative to the host structure and the piezoelectric ceramic, respectively. Substituting Eq. (25) in Eq. (30)

$$\mathrm{T} = \iiint_{V_s} \frac{1}{2}\rho_s \dot{\mathbf{u}}_i^T \mathbf{N}_u^T \mathbf{N}_u \dot{\mathbf{u}}_i dV_s + \iiint_{V_p} \frac{1}{2}\rho_p \dot{\mathbf{u}}_i^T \mathbf{N}_u^T \mathbf{N}_u \dot{\mathbf{u}}_i dV_p \tag{31}$$

The potential energy can be written as the addition of the potential energies of the structure and the piezoelectric material

$$\mathrm{U} = \mathrm{U}_s + \mathrm{U}_p = \iiint_{V_s} \frac{1}{2}\mathbf{S}^T \sigma_s dV_s + \iiint_{V_p} \frac{1}{2}\mathbf{S}^T \sigma_p dV_p \tag{32}$$

where $\boldsymbol{S}$ and σ are the strain and stress tensors, respectively. The constitutive relations of the structure in matrix form

$$\sigma = \mathbf{GS} \ \text{ and } \ \mathbf{G} = \frac{E}{(1+\upsilon)(1-2\upsilon)} \begin{bmatrix} 1-\upsilon & \upsilon & \upsilon & 0 & 0 & 0 \\ \upsilon & 1-\upsilon & \upsilon & 0 & 0 & 0 \\ \upsilon & \upsilon & 1-\upsilon & 0 & 0 & 0 \\ 0 & 0 & 0 & \frac{1-2\upsilon}{2} & 0 & 0 \\ 0 & 0 & 0 & 0 & \frac{1-2\upsilon}{2} & 0 \\ 0 & 0 & 0 & 0 & 0 & \frac{1-2\upsilon}{2} \end{bmatrix} \tag{33}$$

where $\mathbf{G}$ is the matrix that contains the elastic coefficients of the material. E denotes the Young's modulus and υ is the Poisson rate. The strain can be represented in matrix form

$$\mathbf{S} = \mathbf{L}_u \mathbf{u}; \quad \begin{Bmatrix} S_x \\ S_y \\ S_z \\ S_{xy} \\ S_{xz} \\ S_{yz} \end{Bmatrix} = \begin{bmatrix} \frac{\partial}{\partial x} & 0 & 0 \\ 0 & \frac{\partial}{\partial y} & 0 \\ 0 & 0 & \frac{\partial}{\partial z} \\ \frac{\partial}{\partial y} & \frac{\partial}{\partial x} & 0 \\ \frac{\partial}{\partial z} & 0 & \frac{\partial}{\partial x} \\ 0 & \frac{\partial}{\partial z} & \frac{\partial}{\partial y} \end{bmatrix} \begin{Bmatrix} u_x \\ u_y \\ u_z \end{Bmatrix}; \quad \mathbf{S} = \mathbf{L}_u \mathbf{N}_u \mathbf{u}_i \tag{34}$$

or

$$\mathbf{S} = \mathbf{B}_u \mathbf{u}_i \tag{35}$$

and

$$\mathbf{B}_u = \mathbf{L}_u \mathbf{N}_u \tag{36}$$

Substituting Eq. (35) into (33), the stress tensor for the host structure is given by

$$\sigma_s = \mathbf{G}_s \mathbf{S} = \mathbf{G}_s \mathbf{B}_u \mathbf{u}_i \tag{37}$$

Now, substituting equations (35) and (37) in the domain V_s of the Eq. (32)

$$\mathrm{U}_s = \iiint_{V_s} \frac{1}{2} \mathbf{u}_i^T \mathbf{B}_u^T \mathbf{G}_s \mathbf{B}_u \mathbf{u}_i dV_s \tag{38}$$

Similarly to the host structure, the potential energy must be found to the ceramic material. In this work the following linear constitutive relations for piezoelectric materials are employed

$$D = \mathbf{e}^T \mathbf{S} + \in^S \mathbf{E} \quad \text{(Sensor's Equation or Direct Effect)} \tag{39}$$

$$\sigma_p = \mathbf{c}^E \mathbf{S} - \mathbf{e}\mathbf{E} \quad \text{(Actuator's Equation or Inverse Effect)} \tag{40}$$

or

$$\left\{ \begin{array}{c} D_1 \\ D_2 \\ D_3 \end{array} \right\} = \left[\begin{array}{cccccc} 0 & 0 & 0 & 0 & e_{15} & 0 \\ 0 & 0 & 0 & e_{24} & 0 & 0 \\ e_{31} & e_{23} & e_{33} & 0 & 0 & 0 \end{array} \right] \left\{ \begin{array}{c} S_{11} \\ S_{22} \\ S_{33} \\ 2S_{23} \\ 2S_{31} \\ 2S_{12} \end{array} \right\} + \left[\begin{array}{ccc} \in_{11}^S & 0 & 0 \\ 0 & \in_{22}^S & 0 \\ 0 & 0 & \in_{33}^S \end{array} \right] \left\{ \begin{array}{c} \mathrm{E}_1 \\ E_2 \\ E_3 \end{array} \right\} \tag{41}$$

Sensor's Equation: Direct effect

$$\left\{ \begin{array}{c} \sigma_{11} \\ \sigma_{22} \\ \sigma_{33} \\ \sigma_{23} \\ \sigma_{31} \\ \sigma_{12} \end{array} \right\} = \left[\begin{array}{cccccc} c_{11}^E & c_{12}^E & c_{13}^E & 0 & 0 & 0 \\ c_{12}^E & c_{22}^E & c_{23}^E & 0 & 0 & 0 \\ c_{13}^E & c_{23}^E & c_{33}^E & 0 & 0 & 0 \\ 0 & 0 & 0 & c_{44}^E & 0 & 0 \\ 0 & 0 & 0 & 0 & c_{55}^E & 0 \\ 0 & 0 & 0 & 0 & 0 & c_{66}^E \end{array} \right] \left\{ \begin{array}{c} S_{11} \\ S_{22} \\ S_{33} \\ 2S_{23} \\ 2S_{31} \\ 2S_{12} \end{array} \right\} - \left[\begin{array}{ccc} 0 & 0 & e_{31} \\ 0 & 0 & e_{23} \\ 0 & 0 & e_{33} \\ 0 & e_{24} & 0 \\ e_{15} & 0 & 0 \\ 0 & 0 & 0 \end{array} \right] \left\{ \begin{array}{c} \mathrm{E}_1 \\ E_2 \\ E_3 \end{array} \right\} \tag{42}$$

Actuator's Equation: Inverse effect

where the superscript **S** means that the values are measured at constant strain and the superscript **E** means that the values are measured at constant electric field, σ_p is the stress tensor, $\boldsymbol{D}$ is the electric displacement vector, **E** is the electric field, $\mathbf{c}^E$ is the elastic constants at constant electric field, **e** denotes the piezoelectric stress coefficients and $\in^S$ is the dielectric tensor at constant mechanical strain.

The electric field can be written similarly the strain tensor form by

$$\mathbf{E} = \mathbf{L}_{\varphi}\ \varphi \tag{43}$$

where $\mathbf{L}_{\varphi}$ is the matrix that contains the derivative operators. Substituting Eq. (26) into (43)

$$\mathrm{E} = \mathbf{L}_{\varphi}\mathbf{N}_{\varphi}\varphi_i \tag{44}$$

or

$$\mathrm{E} = \mathbf{B}_{\varphi}\varphi_i \tag{45}$$

where

$$\mathbf{B}_{\varphi} = \mathbf{L}_{\varphi}\mathbf{N}_{\varphi} \tag{46}$$

Substituting equations (35) and (45) into (40) (mechanics stress in the PZT), then

$$\sigma_p = \mathbf{c}^E\mathbf{B}_u\mathbf{u}_i - \mathbf{e}\mathbf{B}_{\varphi}\varphi_i \tag{47}$$

Now, substituting equations (35) and (47) in the V_p domain of the Eq. (32) it is obtained

$$\mathrm{U}_p = \iiint\limits_{V_p} \frac{1}{2}\mathbf{u}_i^T\mathbf{B}_u^T\mathbf{c}^E\mathbf{B}_u\mathbf{u}_i dV_p - \iiint\limits_{V_p} \frac{1}{2}\mathbf{u}_i^T\mathbf{B}_u^T\mathbf{e}\mathbf{B}_{\varphi}\varphi_i dV_p \tag{48}$$

The total potential energy of the piezostructure is given by adding equations (38) and (48)

$$\mathrm{U} = \iiint\limits_{V_s} \frac{1}{2}u_i^T\mathbf{B}_u^T G_s B_u u_i dV_s + \iiint\limits_{V_p} \frac{1}{2}u_i^T\mathbf{B}_u^T c^E B_u u_i dV_p - \iiint\limits_{V_p} \frac{1}{2}u_i^T\mathbf{B}_u^T e\mathbf{B}_{\varphi}\varphi_i dV_p \tag{49}$$

The work done by electrical forces is given by

$$\mathrm{W}_e = \iiint\limits_{V_p} \frac{1}{2}\mathrm{E}^T D dV_P \tag{50}$$

where $\boldsymbol{D}$**,** the electric displacement vector of the PZT, is obtained substituting equations (35) and (45) into Eq. (39)

$$D = \mathbf{e}^T\mathbf{B}_u\mathbf{u}_i + \in^S \mathbf{B}_{\varphi}\varphi_i \tag{51}$$

Now, substituting equations (45) and (51) in Eq. (50), on obtain

$$\mathrm{W}_e = \iiint\limits_{V_P} \frac{1}{2}\varphi_i^T\mathbf{B}_{\varphi}^T\mathbf{e}^T\mathbf{B}_{\mathbf{u}}\mathbf{u}_i dV_P + \iiint\limits_{V_P} \frac{1}{2}\varphi_i^T\mathbf{B}_{\varphi}^T \in^S \mathbf{B}_{\varphi}\varphi_i dV_P \tag{52}$$

Substituting equations (31), (49) and (52) into (29), one obtain the Lagrangian as

$$\begin{aligned} \mathrm{L} = & \iiint_{V_s} \tfrac{1}{2}\rho_s \dot{\mathbf{u}}_i^T \mathbf{N}_u^T \mathbf{N}_u \dot{\mathbf{u}}_i dV_s + \iiint_{V_p} \tfrac{1}{2}\rho_p \dot{\mathbf{u}}_i^T \mathbf{N}_u^T \mathbf{N}_u \dot{\mathbf{u}}_i dV_p - \iiint_{V_s} \tfrac{1}{2}\mathbf{u}_i^T \mathbf{B}_u^T \mathbf{G}_s \mathbf{B}_u \mathbf{u}_i dV_s - \\ & \iiint_{V_p} \tfrac{1}{2}\mathbf{u}_i^T \mathbf{B}_u^T \mathbf{c}^E \mathbf{B}_u \mathbf{u}_i^d V_p + \iiint_{V_p} \tfrac{1}{2}\mathbf{u}_i^T \mathbf{B}_u^T \mathbf{e}\ \mathbf{B}_\varphi \varphi_i dV_p + \iiint_{V_p} \tfrac{1}{2}\varphi_i^T \mathbf{B}_\varphi^T\ \mathbf{e}^T \mathbf{B}_u \mathbf{u}_i^d V_p + \\ & \iiint_{V_p} \tfrac{1}{2}\varphi_i^T \mathbf{B}_\varphi^T\ \in^S\ \mathbf{B}_\varphi \varphi_i dV_p \end{aligned} \tag{53}$$

Appling Lagrange's Equation in (53) for the generalized velocity, on obtain

$$\frac{\partial \mathrm{L}}{\partial \dot{\mathbf{u}}_i} = \left(\iiint_{V_s} \rho_s \mathbf{N}_u^T \mathbf{N}_u dV_s \right) \dot{\mathbf{u}}_i^+ \left(\iiint_{V_p} \rho_p \mathbf{N}_u^T \mathbf{N}_u dV_p \right) \dot{\mathbf{u}}_i \tag{54}$$

$$\frac{\partial}{\partial t}\left(\frac{\partial \mathrm{L}}{\partial \dot{\mathbf{u}}_i} \right) = \left(\iiint_{V_s} \rho_s \mathbf{N}_u^T N_u dV_s \right) \ddot{\mathbf{u}}_i + \left(\iiint_{V_p} \rho_p \mathbf{N}_u^T \mathbf{N}_u dV_p \right)\ \ddot{\mathbf{u}}_i \tag{55}$$

or

$$\frac{\partial}{\partial t}\left(\frac{\partial \mathrm{L}}{\partial \dot{\mathbf{u}}_i} \right) = \mathbf{M}_s^e \ddot{\mathbf{u}}_i^+ \mathbf{M}_p^e \ddot{\mathbf{u}}_i \tag{56}$$

where $\mathbf{M}_s^e$ and $\mathbf{M}_p^e$ are the elementary matrices (local) of mass of the host structure and of the PZT, respectively that are given by

$$\mathbf{M}_s^e = \iiint_{V_s} \rho_s \mathbf{N}_u^T \mathbf{N}_u dV_s \tag{57}$$

$$\mathbf{M}_p^e = \iiint_{V_p} \rho_p \mathbf{N}_u^T \mathrm{N}_u dV_p \tag{58}$$

Now, applying Lagrange's Equation for the generalized displacement

$$\begin{aligned} \tfrac{\partial \mathrm{L}}{\partial \mathbf{u}_i} = & -\left(\iiint_{V_s} \mathbf{B}_u^T \mathbf{G}_s \mathbf{B}_u^d V_s \right)\ \mathbf{u}_i^- \left(\iiint_{V_p} \mathbf{B}_u^T \mathbf{c}^E \mathbf{B}_u dV_p \right)\ \mathbf{u}_i^+ \\ & \left(\iiint_{V_p} \tfrac{1}{2}\mathbf{B}_u^T \mathbf{e} \mathbf{B}_\varphi dV_p \right) \varphi_i + \left(\iiint_{V_p} \tfrac{1}{2}\mathbf{B}_\varphi^T \mathbf{e}^T \mathbf{B}_u dV_p \right) \varphi_i^T \end{aligned} \tag{59}$$

or

$$\frac{\partial \mathrm{L}}{\partial u_i} = -\mathbf{K}_s^e u_i - \mathbf{K}_p^e u_i + \mathbf{K}_{u\varphi}^e \varphi_i \tag{60}$$

where $\mathbf{K}_s^e$ and $\mathbf{K}_p^e$ are local stiffness matrices of the host structure and of the PZT, respectively, and $\mathbf{K}_{u\varphi}^e$ is the electrical-mechanical coupling stiffness matrix. These matrices are given by

$$\mathbf{K}_s^e = \iiint_{V_s} \mathbf{B}_u^T \mathbf{G}_s \mathbf{B}_u^d V_s \tag{61}$$

$$\mathbf{K}_p^e = \iiint_{V_p} \mathbf{B}_u^T \mathbf{c}^E \mathbf{B}_u dV_p \tag{62}$$

$$\mathbf{K}_{u\varphi}^e = \iiint_{V_p} \mathbf{B}_u^T e \mathbf{B}_\varphi dV_p \tag{63}$$

Appling Lagrange's Equation for the electric potential, one obtain

$$\frac{\partial}{\partial t}\left(\frac{\partial \mathrm{L}}{\partial \dot{\phi}_i}\right) = 0 \tag{64}$$

$$\frac{\partial \mathrm{L}}{\partial \phi_i} = \left(\iiint_{V_p} \frac{1}{2}\mathbf{B}_u^T \mathbf{e} \mathbf{B}_\varphi dV_p\right) \mathbf{u}_i^+ \left(\iiint_{V_p} \frac{1}{2}\mathbf{B}_\varphi^T \mathbf{e}^T \mathbf{B}_u dV_p\right) \mathbf{u}_i^+ \left(\iiint_{V_p} \mathbf{B}_\varphi^T \in^S \mathbf{B}_\varphi dV_p\right) \phi_i \tag{65}$$

or

$$\frac{\partial \mathrm{L}}{\partial \varphi_i} = \mathbf{K}_{\varphi u}^e u_i + \mathbf{K}_{\varphi\varphi}^e \phi_i \tag{66}$$

where $\mathbf{K}_{\varphi u}^e$ is the electrical-mechanical coupling stiffness matrix and $\mathbf{K}_{\varphi\varphi}^e$ the dielectric stiffness matrix. These matrices are given by

$$\mathbf{K}_{\varphi u}^e = \iiint_{V_p} \mathbf{B}_\varphi^T \mathbf{e}^T \mathbf{B}_u dV_p \tag{67}$$

$$\mathbf{K}_{\varphi\varphi}^e = \iiint_{V_P} \mathbf{B}_\varphi^T \in^S \mathbf{B}_\varphi^d V_P \tag{68}$$

It can be observed from equations (63) and (67) that $\mathbf{K}_{\varphi u}^e = \left(\mathbf{K}_{u\varphi}^e\right)^T$. Equations (57), (58), (61), (62), (63), (67) and (68) are integrated, getting thus the local matrices. Substituting these equations into (27) and (28) the matrices of elements can be written as

$$\begin{cases} \left(\mathbf{M}_s^e + \mathbf{M}_p^e\right) \ddot{u}_i + \left(\mathbf{K}_s^e + \mathbf{K}_p^e\right) \mathrm{u}_i - \left(\mathbf{K}_{u\varphi}^e\right) \varphi_i = \mathbf{F}^e \\ -\left(\mathbf{K}_{\varphi u}^e \varphi_i + \mathbf{K}_{\varphi\varphi}^e \varphi_i\right) = \mathbf{Q}^e \end{cases} \tag{69}$$

From the technique of finite elements, the global matrices are mounted. The global system of motion equations of a piezostructure with the incorporated electrical-mechanical coupling effect is

$$\begin{bmatrix} \mathbf{M}_{uu} & 0 \\ 0 & 0 \end{bmatrix} \begin{Bmatrix} \ddot{\mathbf{u}} \\ \ddot{\varphi} \end{Bmatrix} + \begin{bmatrix} \mathbf{K}_{uu} & \mathbf{K}_{u\varphi} \\ \mathbf{K}_{\varphi u} & \mathbf{K}_{\varphi\varphi} \end{bmatrix} \begin{Bmatrix} \mathbf{u} \\ \varphi \end{Bmatrix} = \begin{Bmatrix} \mathbf{F} \\ \mathbf{Q} \end{Bmatrix} \tag{70}$$

where the global matrices are defined by

$$\mathbf{M}_{uu} = \sum_{i=1}^{ne} \left(\mathbf{M}_s^e\right)_i + \sum_{j=1}^{np} \left(\mathbf{M}_p^e\right)_j \tag{71}$$

$$\mathbf{K}_{uu} = \sum_{i=1}^{ne} (\mathbf{K}_s^e)_i + \sum_{j=1}^{np} (\mathbf{K}_p^e)_j \tag{72}$$

$$\mathbf{K}_{u\varphi} = -\sum_{j=1}^{np} (\mathbf{K}_{u\varphi}^e)_j \tag{73}$$

$$\mathbf{K}_{\varphi\varphi} = -\sum_{j=1}^{np} (\mathbf{K}_{\varphi\varphi}^e)_j \tag{74}$$

where *ne* is the number of elements of the host structure and *np* the number of PZTs inserted in the structure. The symbol of addition in the above equations means the conventional finite element assembly.

Structures in general present a certain degree of damping. This degree is difficult of being defined with precision, but it can be estimated. In this work, it is considered that the damping $\mathbf{D}_a$ is proportional to the mass and the stiffness. Many authors show in details that structures with small non proportional damping can be approached by proportional damping without causing significant errors [1].

The algorithm for damage location in a flexible plate is present bellow in a schematic way:

1. Obtain the dynamic model of second order by finite elements for the structure without damage;
2. Transform to modal domain;
3. Use the space of states realization;
4. Calculate H_2 and H_∞ norms of the system considering two first modes (it is possible to consider all the structural modes, however, it can increase the computational time);
5. Calculate H_2 and H_∞ norms for each mode, considering all sensors;
6. Obtain the dynamic model of second order by finite elements for the structure with damage;
7. Repeat steps 2, 3, 4 and 5 for the structure with damage;
8. Calculate the sensor index using H_2 and H_∞ norms obtained in steps 4 and 7, as show equations 17 and 23;
9. Calculate modal index using H_2 and H_∞ norms obtained in steps 5 and 7, as show equations 18 and 24.

6 Numerical application

The proposed methodology will be verified in a plate structure. For practical situations, the system norms can be obtained directly from the measured signals, as for instance, the matrices **A**, **B**, **C** and **D** can be estimated through eigensystem realization algorithm (ERA). In the following application, the matrices of mass and stiffness are described using the theory of Kirchhoff plate. The theory statements that a normal plan to the neutral axis before the strain remains normal to the neutral axis after the deformation, Fig. 1.

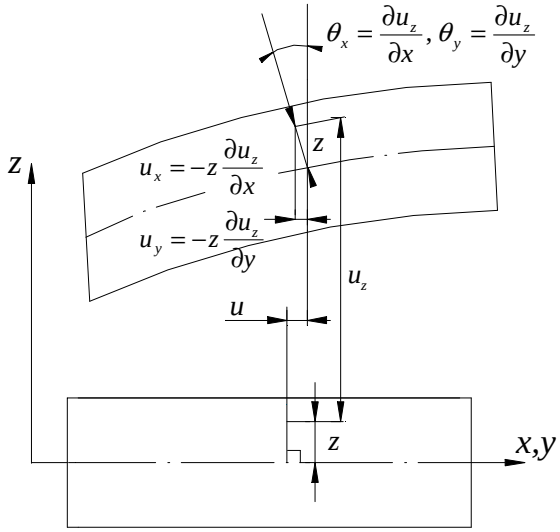

Figure 1: Displacement of points on normal lines to the plans xz and yz.

Consequently, the following relations of displacement can be written

$$\begin{aligned} u_x &= -z\frac{\partial u_z}{\partial x} \\ u_y &= -z\frac{\partial u_z}{\partial y} \\ u_z &= u_z(x,y) \end{aligned} \tag{75}$$

the strain can be written in terms of the transversal displacements u_z, [14]

$$\begin{aligned} S_x &= \frac{\partial u_x}{\partial x} = -z\frac{\partial^2 u_z}{\partial x^2} \\ S_y &= \frac{\partial u_y}{\partial y} = -z\frac{\partial^2 u_z}{\partial y^2} \\ S_{xy} &= \frac{\partial u_x}{\partial y} + \frac{\partial u_y}{\partial x} = -2z\frac{\partial^2 u_z}{\partial x \partial y} \end{aligned} \tag{76}$$

The modeling considers an element of plate with four nodes and three structural degrees of freedom per node (transversal displacement u_z in direction z, rotation θ_x around axis x, and rotation θ_y around axis y) and one electrical degree of freedom per node (electric potential$\phi_)$.

The displacement vector $\mathbf{u}_i$and electric potentialφ_i of the element are written as

$$\begin{aligned} \mathbf{u}_i &= [u_{z1}\ \theta_{x1}\ \theta_{y1}\ u_{z2}\ \theta_{x2}\ \theta_{y2}\ u_{z3}\ \theta_{x3}\ \theta_{y3}\ u_{z4}\ \theta_{x4}\ \theta_{y4}]^T \\ \varphi_i &= [\phi_1\ \phi_2\ \phi_3\ \phi_4] \end{aligned} \tag{77}$$

The positive directions are indicated in figure 2.

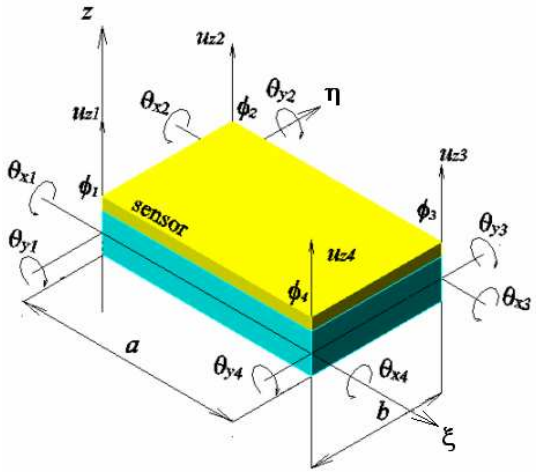

Figure 2: Rectangular structural element with electromechanical coupling.

where ξ and η are generalized coordinates of the element in function, respectively, of global coordinates x and y. The length and the width of the element are $a$and b, respectively. The interpolation function, $\mathbf{N}_u$, for displacement in the plate element has the form [14]

$$\mathbf{N}_\mathbf{u}^T = \begin{bmatrix} 1-\xi\eta-(3-2\xi)\xi^2(1-\eta)-(1-\xi)(3-2\eta)\eta^2 \\ (1-\xi)\eta(1-\eta)^2 b \\ -\xi(1-\xi)^2(1-\eta)a \\ (1-\xi)(3-2\eta)\eta^2+\xi(1-\xi)(1-2\xi)\eta \\ -(1-\xi)(1-\eta)\eta^2 b \\ -\xi(1-\xi)^2\eta a \\ (3-2\xi)\xi^2\eta-\xi\eta(1-\eta)(1-2\eta) \\ -\xi(1-\eta)\eta^2 b \\ (1-\xi)\xi^2\eta a \\ (3-2\xi)\xi^2(1-\eta)+\xi\eta(1-\eta)(1-2\eta) \\ \xi\eta(1-\eta)^2 b \\ (1-\xi)\xi^2(1-\eta)a \end{bmatrix} \tag{78}$$

The interpolation function for electric potential, $\mathbf{N}_\varphi$, is considered as

$$\mathbf{N}_\varphi = \begin{bmatrix} 1-\xi-\eta+\xi\eta \\ \eta-\xi\eta \\ \xi\eta \\ \xi-\xi\eta \end{bmatrix}^T \tag{79}$$

Substituting the variable functions and the piezoceramic patch properties, in the corresponding equations, defined in the former section, one can get the final motion equations written in the state space form as defined in Eq. (1).

An aluminum plate, as shown in Fig. 3, was considered to verify the proposed methodology. The plate is discretized by FEM in 100 elements and 363 structural dof's (121 nodes). The plate is clamped in one end, so considering this boundary condition, the system has N=660 states. Table 1 shows the physic and geometric properties of the plate used in the FEM modeling.

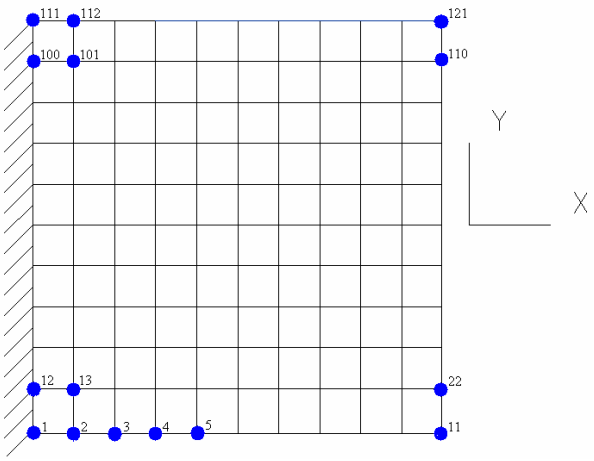

Figure 3: Finite element model for a cantilever plate.

Table 1: Geometric and physic properties of the plate.

Dimensions (m)	Length	Width	Thickness
	0.5	0.03	0.005
Density (kg.m^{-3})	2710		
Young's Modulus (GPa)	70		

Four damage cases were analyzed. The first one considers 10% of reduction in the stiffness of the element 6, the second one 20% of reduction in the stiffness of the element 18, the third one 30%

of reduction in the stiffness of the element 22, and fourth one 20% of reduction in the stiffness in elements 3 and 20. The concept of this methodology requires a measurement points for each region under analysis. For practical situations is not necessary the monitoring of every element. The engineer must choose some probable positions to occur damages. This application, only to verify the sensitivity of each sensor position, considers PVDF sensors placed in first thirty element positions. A vertical force (F), representing a disturbance, was applied in – Z direction in the free end of the plate, Fig. 4.

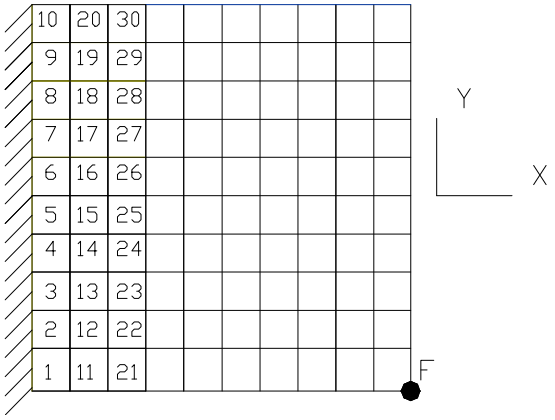

Figure 4: Schematic picture showing the position of thirty PVDF sensors and the point of application of the disturbance force (F).

Figure 5 shows the indices of the sensor for the first case of damage calculated with H_2 norm, and Fig. 6 shows the indices calculated with H_∞ norm. One observes clearly that the structural damage was located in element 6 for both approaches. In Fig. 7 it can be observed that mode 1 is mostly affected by this damage.

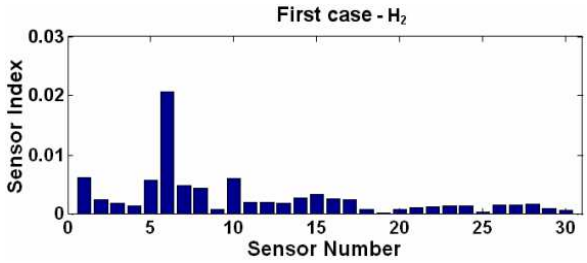

Figure 5: H_2 Sensor Indices for damage in element 6, first case.

Figure 8 shows the indices of the sensor for the second case of damage calculated with H_2 norm, while Fig. 9 shows the indices calculated with H_∞ norm. It can be observed that in this case the sensor indices showed the region of damage location in both approaches, Fig. 10. In Fig. 11 it can be observed that mode 1 is mostly affected by the damage.

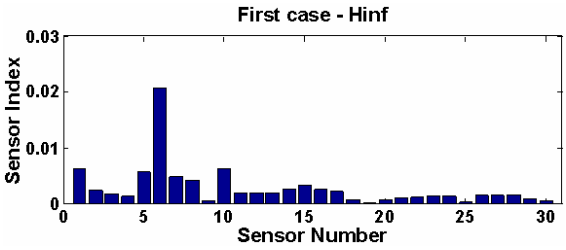

Figure 6: H_∞ Sensor Indices for damage in element 6, first case.

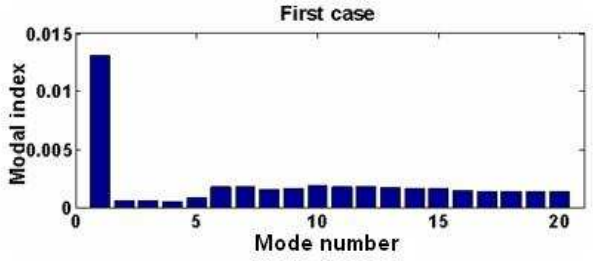

Figure 7: Modal Indices for damage in element 6, first case.

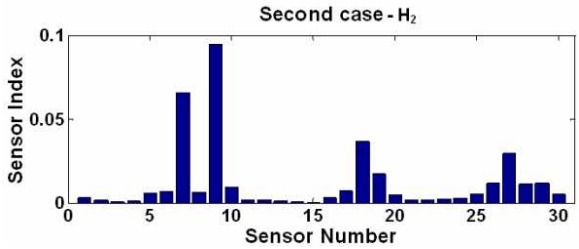

Figure 8: H_2 Sensor Indices for damage in element 18, second case.

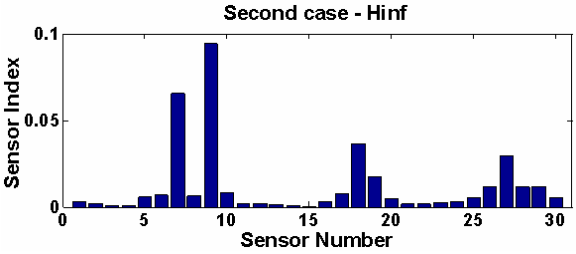

Figure 9: H_∞ Sensor Indices for damage in element 18, second case.

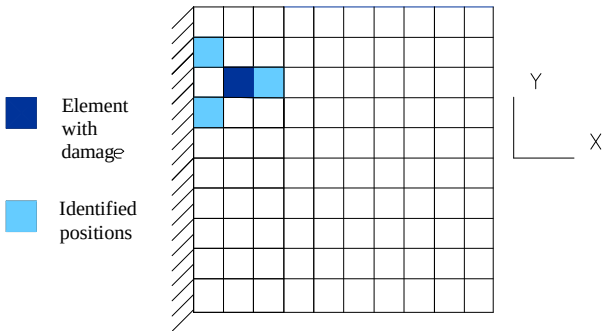

Figure 10: Region of damage identified by sensor indices for the second case.

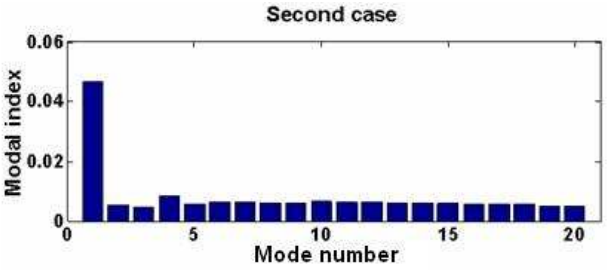

Figure 11: Modal Indices for damage in element 18, second case.

Similarly, figure 12 shows the sensor indices for the third case of damage calculated with H_2 norm, while Fig. 13 shows the indices calculated with H_∞ norm. The structural damage was located in element 22, but both approaches also identified a probable damage in element 2, 11, and 21; Fig. 14 shows the position of these elements. In Fig. 15, one can observe that mode 1 is mostly affected by this damage.

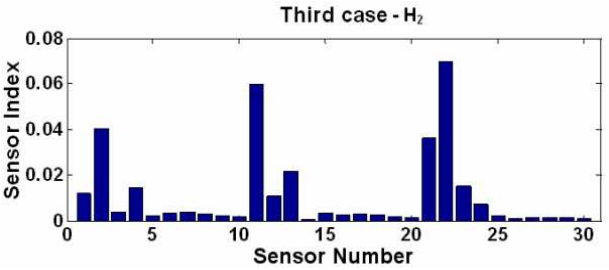

Figure 12: H_2 Sensor Indices for damage in element 22, third case.

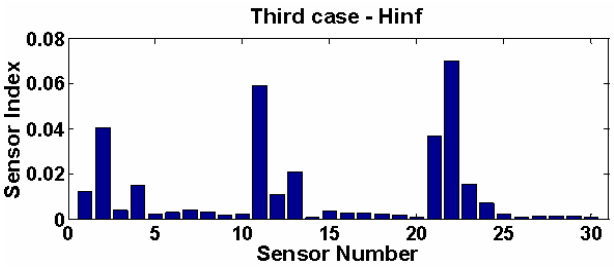

Figure 13: H_∞ Sensor Indices for damage in element 22, third case.

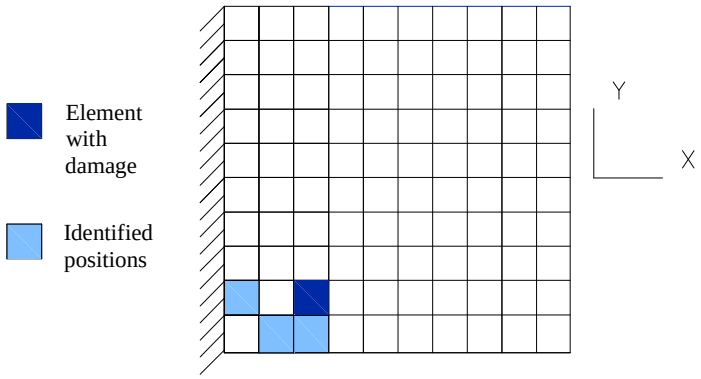

Figure 14: Region of damage identified by sensor indices for the third case.

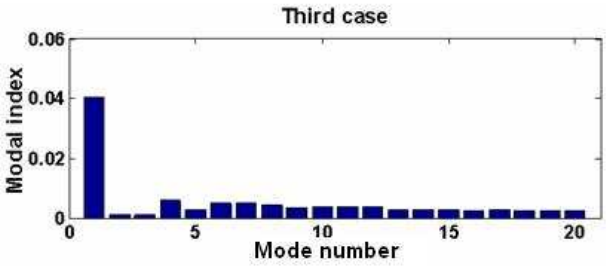

Figure 15: Modal Indices for damage in element 22, third case.

In the fourth case are simulated simultaneous damages in two elements. Figure 16 shows the sensor indices calculated with H_2 norm, while Fig. 17 shows the indices calculated with H_∞ norm. It can be observed that the damage in element 20 was clearly identified, as well as a region of damage near of element 3, Fig. 18. In Fig. 19, it can be observed that mode 1 is mostly affected by these simultaneous damages.

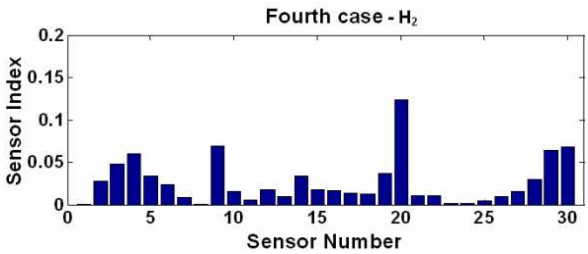

Figure 16: H_2 Sensor Indices for damage in elements 3 and 20, fourth case.

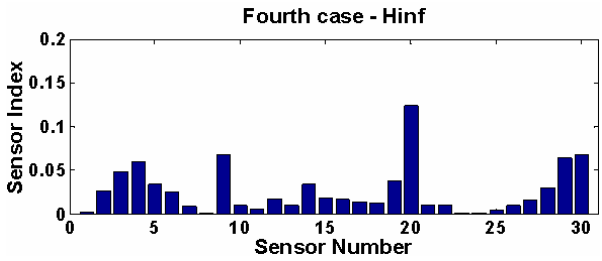

Figure 17: H_∞ Sensor Indices for damage in elements 3 and 20, fourth case.

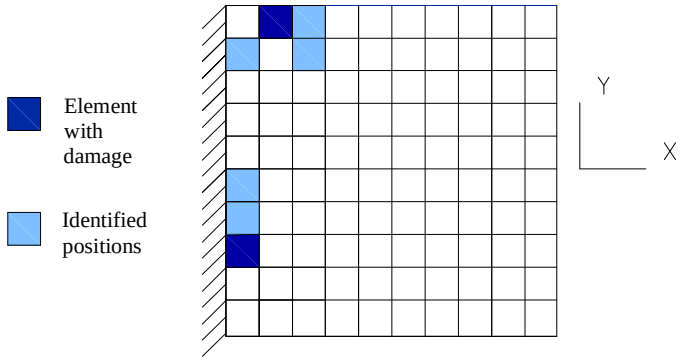

Figure 18: Region of damage identified by sensor indices for the fourth case.

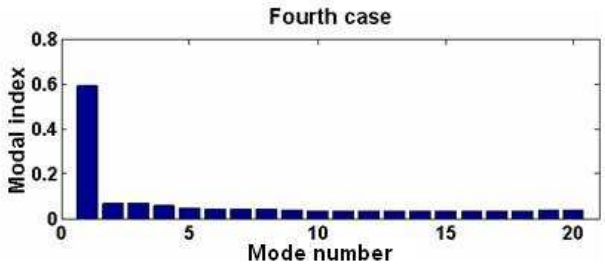

Figure 19: Modal Indices for simultaneous damages in elements 3 and 20, fourth case.

7 Final remarks

Structural systems are susceptible of structural damage over their operating lives from impact, operating loads, and fatigue. Identifying the location of structural damage leads to improved safety and offers the possibility of extending the service life of the structure by repairing components only when necessary.

The advances in the instrumentation area, new material and advanced techniques in the last years have had a great impact in new damage location proposals. The continuous growth of the use of new materials to make lighter and stronger structures and projects of intelligent maintenance, that will only effect the repair if really necessary, can economically be attractive. Therefore, the methodology for structural damage detection using system norms is an important approach that must be considered, since it is of easy evaluation and computational implementation. In despite of these features, there are a small number of related papers in the literature using system norms to locate damages. The authors do not know experimental work using the proposed approach, so, it must be the next step. It is worth to mention that one of the most important feature of this technique is the possibility of identify simultaneous damage locations.

Acknowledgements: The authors acknowledge the support of the Research Foundation of the State of São Paulo (FAPESP-Brazil, process number 04/08731-5).

References

[1] Bhaskar A. Estimates of error in the frequency response of non-classically damped systems. *Journal of Sound and Vibration*, 184:59–12, 1995.

[2] Preumont A., François A., De Man P., and Loix N. A novel electrode concept for spatial filtering with piezoelectric films. In *In: Active 2002 – The 2002 International Symposium on Active Control of Sound and Vibration*, Institute of Sound and Vibration Research; University of Southampton, Southampton, United Kingdom, 2002.

[3] Zubaydi A., Haddara M.R., and Swamidas A.S.J. *Damage Identification in a Ship's Structure Using Neural Networks*, volume 29. Ocean Engineering, 2002.

[4] Mustafa D. and Glover K. Controller reduction by h_∞ balanced truncation. *IEEE Transactions on automatic control - AC-36*, pages 668–682, 1991.

[5] Wang D.H. and Huang S.L. Health monitoring and diagnosis for flexible structures with pvdf piezoelectric film sensor array. *ournal of Intelligent Material Systems and Structures*, 2:482–491, 2000.

[6] Ewins D.J. *Modal Testing*. Wiley, New York, 1984.

[7] Inman D.J. Smart structures: Examples and new problems. In *XVI Brazilian Congress of Mechanics Engineering – COBEM*, pages 26–30, Uberlândia, MG; Brazil, 2001.

[8] Mahmoud H., Kabamba P.T., Ulsoy A.G., and Brusher G.A. Target reduction and balancing using system norms. In *ACC 2002*, 2002.

[9] Panossian H., Gawronski W., and Ossman J. Balanced shaker and sensor placement for modal testing of large flexible structures. In *IMAC-XVI*, Santa Barbara, CA, 1998.

[10] Burl J.B. *Linear Optimal Control: H_2 and H_∞ Methods*. Addison-Wesley, 1999.

[11] Lew J.S. and Juang J.N. Structural damage detection using virtual passive controllers. *Journal of Guidance, Control, and Dynamics*, 25(3):419–424, 2002.

[12] Maia N. and Silva J. et others. *Theoretical and Experimental Modal Analysis*. Research Studies Press Ltd., Baldock, Hertfordshire, England, 1996.

[13] Clark R.L., Saunders W.R., and Gibbs G.P. *Adaptive Structures: Dynamics and Control*. John Wiley & Sons, Inc, 1998.

[14] Timoshenko S.P. and Goodier J.N. *Theory of Elasticity*. McGraw-Hill, 1970.

[15] Hall S.R. and T.J. Conquest. The total data integrity initiative—structural health monitoring, the next generation. In *Proceedings of the USAF ASIP*, volume 2, 1999.

[16] Gatulli V. and Romeo F. Structural identifiability enhancement via feedback. In *Third World Conference on Structural Control*, volume 2, pages 95–100, Como, Italy, 2003.

[17] Lopes Jr. V., Park G., Cudney H.H., and Inman D.J. Impedance based structural health monitoring with artificial neural network. *Journal of Intelligent Material System and Structures*, 11(3):206–214, 2000.

[18] Piéfort V. and Henrioulle K. Modelling of smart structures with collocated piezoelectric actuator/sensor pairs: Influence of the in-plane components. In *5th International Conference on Computational Structures Technology*, Leuven, Belgium, 2000.

[19] Gawronski W. *Dynamics and Control of Structures, A Modal Approach*. Springer Verlag, New York, 1998.

[20] Gawronski W. and Juang J.N. Model reduction for flexible structures. In C.T. Leondes, editor, *Control and dynamics systems science*, volume 36. Academic Press, 1990.

[21] Gawronski W. and Sawicki J.T. Structural damage detection using modal norms. *Journal of Sound and Vibration*, pages 194–198, 2000.